

# Failure in wood related to decay weight losses

about the levels of decay that could be accommodated for certain applications. For example, it has not been possible

John A. Akande

## Abstract

The progressive effects of fungal decay on wood failure morphology were studied, using *Populus tremuloides* Michx. as the fungal substrate. The degree of decay was indexed by loss of wood weight. Decayed and control specimens were stressed to failure prior to macroscopic and ultrastructural analyses of the fracture surfaces. Results showed that fungal decay affected fracture morphology in wood. The nature of the fracture surface reflects the degree of degradation of wood cells. Decayed wood ( $> 2\%$  weight loss) failed differently than sound wood. High-energy fracturing, like splintering and production of rough shear planes, typified the failure characteristics up to 2 percent weight loss. The associated fractographic features included transwall failure of fibers at angles close to the S2 microfibrillar orientation, intra wall failures at the S1/S2 interfaces, and cellular unwinding due to pullout of the S2 wall layer from the whole fiber. These features diminished gradually as weight loss increased. At  $\sim 10$  percent weight loss, failures were often brash and accompanied by abrupt transwall failure of fibers along the transverse plane. The S2 microfibrillar angle did not control the plane of fiber failure in decayed cells. Longitudinal split failures along the parenchyma cells were frequently noted on specimens decayed by white rot fungi. Such failures were initiated at weight losses lower than those required to produce middle lamella separation.

Advanced fungal decay is known to cause low energy (brash) failure in wood (4,10,12). What is not clearly understood are the minute wood deformation patterns culminating in brashness. This knowledge requires a progressive failure analysis of wood as it decays. This could be valuable in modeling a structural use of wood in environments conducive to fungal decay. Field evaluation of wood's load-carrying capacities under the influence of decay has been largely qualitative, giving the engineer little flexibility in designing for wood decay. Uncertainties exist

brown rot (7) and middle lamella separation at the microscopic level from selective delignifiers (9). In order to obtain various deformation patterns, three different fungi were utilized. These were a brown rotter, *Gloeophyllum trabeum* (Fr.) Murrill, (SUNY ESF ,32); *Trametes versicolor* (L.:Fr) Pilat (SUNY ESF,40), which causes simultaneous white rot; and *Bjerkandera adusta* CWilld.:Fr) Karst. (SUNY ESF,58), which can cause a selective white rot. These fungi were used to decay wood samples to different weight loss levels before mechanical failure and ultra-structural analyses. They were obtained in pure culture from SUNY, College of Environmental Science and Forestry, Microbiology Laboratory, Syracuse, N.Y.

#### Experimental procedure

Defect-free wood samples were machined for a tension parallel-to-grain test (5 in. by 0.188 in. by 0.094 in.) and a toughness test (0.5 in. by 0.5 in. by 6 in.) from freshly cut, kiln-dried sapwood of *Populus tremuloides* Michx. Sapwood was utilized to obtain a fast rate of wood decay.

to quantitatively specify the level at which decay in wood products can be halted, using agricultural fumigants to retain adequate residual strength. This is a problem that demands an understanding of the order of occurrences leading to failure and a correlation of this order to a measurable parameter. The objective of this study was to investigate wood deformation patterns at different stages of decay. Weight loss was used as the decay index. Extensive data indicate strong positive relationships between weight loss and strength loss (5,11,13).

Deformation patterns attributed to fungal decay in wood include cubical checks at the macroscopic level from

The author is a Research Assistant Professor, Appalachian Hardwood Center, Div. of Forestry, West Virginia Univ., Morgantown WV 26506-6125. This report was prepared from the results of research conducted as part of the author's doctoral thesis at SUNY, CESF, Syracuse, N.Y. Special thanks to Jack E. Coster for supporting the publication of this paper. This paper was received for publication in August 1989.

© Forest Products Research Society 1990.  
Forest Prod. J. 40(7/8):47-53.

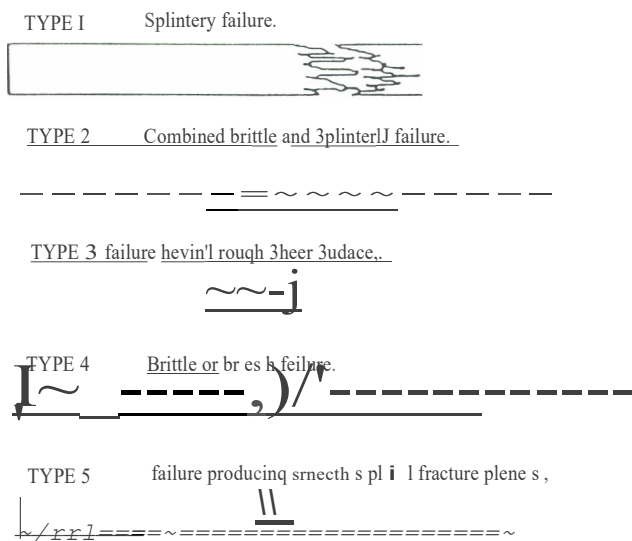


Figure 1. - Schematics of the macroscopic failure patterns.

Tension and toughness tests were adopted to study failure patterns under pure and mixed-mode testing, respectively.

The experimental design was to examine failure characteristics associated with one brown-rotter and two white-rot fungi. Wood samples and their matching controls were subjected to the same treatments, except for fungal exposure. There were 15 test samples per treatment. All the test samples and trial samples were oven-dried to constant weights at 103°C. The dry weights were measured to the nearest 0.01 g. The moisture content (MC) of the samples was adjusted to levels above fiber saturation point (50% through 70% MC). This was followed by specimen sterilization for 30 minutes in an autoclave set at 121°C and a pressure of 15 psi.

Decay chambers were set up in a laboratory room at 28°C, using 32-ounce French square bottles, into which a malt extract-agar (MEA) medium was prepared. Fungal growth in the culture medium was allowed for 2 weeks before test specimens were positioned on the culture. Control chambers containing MEA were not inoculated with fungus. Decay experiments ranged from 9 days to 10 weeks to obtain target weight losses. Weight loss was monitored intermittently, through trial samples, to determine the approximate range of weight loss.

At any target weight loss, specimens were assembled and tested to failure. Tension tests were performed on a floor model TTB Instron machine. A USDA Forest Products Laboratory testing machine was used to test the toughness samples. Macroscopic failure types were identified and classified into five main categories (Fig. 1). Failure-type frequency data were recorded separately for tension and toughness specimens. Data for control and decayed specimens were later compared to determine any significant difference.

Upon specimen failure, fracture surfaces were carefully removed with a razor blade and mounted on scanning electron microscope (SEM) specimen studs. A Technics sputter coater was used to goldcoat the fracture surfaces.

TABLE 1. - Distribution of failure types in tension parallel to grain.

Weight loss (%)	Failure type	Occurrence of failure types (Decayed minus control) <sup>a</sup>			
		Control	<i>T. verso</i>	<i>B. adusta</i>	<i>G. trab.</i>
2	1	67	7	-7	0
	3	33	-13	7	-13
	4	0	7	0	13
5	5	0	0	0	0
	1	60	20	-27	-40
	3	40	-20	-40	0
10	4	0	0	40	40
	5	0	0	27	0
	1	60	-33	-33	-40
16	3	40	-40	-40	-13
	4	0	40	33	53
	5	0	33	40	0

<sup>a</sup> Sample size is 15. Figure 1 contains a description of the failure types. Type 2 failure was not observed in the tension stressing. Negative values denote fewer failures in decayed than in control specimens.

<sup>b</sup> Difference between percent occurrence of failure type in decayed and control specimens.

TABLE 2. - Distribution of failure types under toughness test.

Weight loss (%)	Failure type	Occurrence of failure types (Decayed minus control) <sup>a</sup>			
		Control	<i>T. verso</i>	<i>B. adusta</i>	<i>G. trab.</i>
2	1	40	17	20	0
	2	33	-20	7	-7
	3	27	-7	0	-27
6	4	0	0	0	20
	5	0	0	0	0
	1	4	0	-47	-47
10	2	4	-20	7	-7
	3	1	-13	-13	34
	4	0	13	27	20
16	5	0	20	27	0
	1	6	-53	-47	-47
	2	0	0	-6	7
10	3	7	20	13	40
	4	0	33	40	0

<sup>a</sup> Sample size is 15. Figure 1 contains a description of the failure types. Negative values denote fewer failures in decayed than in control specimens.

<sup>b</sup> Difference between percent occurrence of failure type in decayed and control specimens.

SEM observations, particularly for decayed samples, were double-checked with a Nikon light microscope with epi-illumination attachments. To do this, samples with the same decay level as those observed under the SEM were microtome-sectioned to a thickness of 20 μm, mounted on a glass slide, and stained with hematoxylin and safranin.

## Results

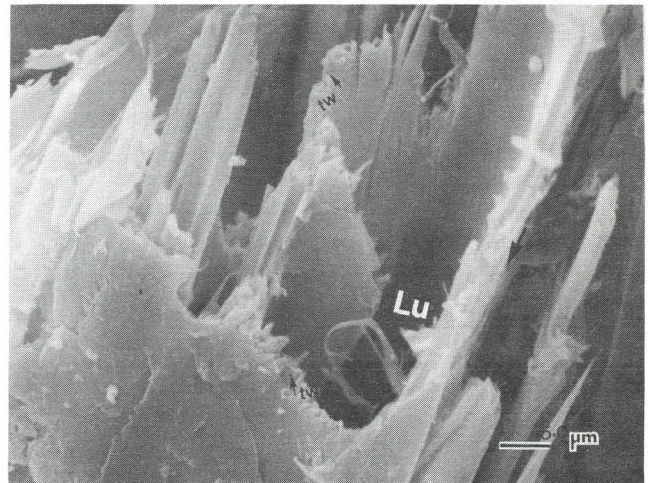
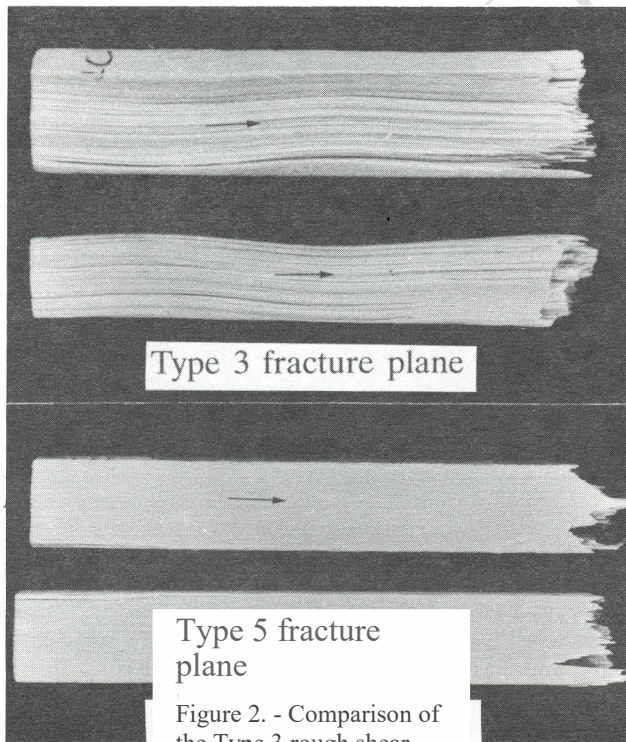
### Macroscopic failures

A summary of the macroscopic failure data is presented in Tables 1 and 2. Failure type frequency data were recorded at 2, 5, 10, and 16 percent target weight loss for the tension specimens; and at 2, 6, and 10 percent weight loss for the toughness specimens. The toughness spec-

2. mens did not decay to 16 percent weight loss during the 10-week incubation period set for this experiment. In the control tension specimens, the most common modes of failure were Types 1 and 3. The effects of decay were small or absent at 2 percent weight loss. Beyond this level, Type 4 and 5 failures gradually set in. A similar trend occurred under toughness testing. Generally, a high frequency of Type 4 and 5 failures were reached in white-rotted specimens with a 6 to 10 percent weight loss. No Type 5 failure occurred in wood decayed by *Gloeophyllum trabeum*, but this fungus attained a considerable frequency of Type 4 failure at weight losses of 10 and 16 percent. As opposed to specimens tested for toughness, Type 2 failure did not occur in tension specimens - only Types 1, 3, 4, and 5. To remove any ambiguity in differentiating Type 3 and 5 failures, the topography of their fracture planes are contrasted in Figure 2. Results showed that the Type 3 failure is characterized by rugged fracture planes in contrast to the smooth fracture planes typical of Type 5 failure. Type 5 failure occurred in both tension and toughness specimens decayed by *Bjerkandera adusta* and *Trametes versicolor*. Type 5 failure was first recognized in wood samples decayed by *Bjerkandera adusta* at a 5 percent weight loss. Similar observations were recorded in samples decayed by *Trametes versicolor* at a 6 percent weight loss.

In the control toughness specimens, Types 1, 2, and 3 failures were most common. Where Type 2 failure occurred, the brittle component was located on the compression side of the toughness specimens, while the tension side contained much of the splintery components. Only Type 2 failure appeared to distinguish toughness from tension

split) fracture plane typical of white-rot degradation. Type 5 fracture plane is less rugged in appearance compared to Type 3.



fracture plane (arrow) in sound wood with Type 5 (longitudinal smooth

failure patterns. Toughness failures revealed that the side of the specimens that were impact-loaded produced compression ridges (Fig. 3) from cells that buckled in this area. Type 5 failure in toughness testing was also unique to white rot and Type 5 failures increased as weight loss increased. At 10 percent weight loss, the frequency of Type 4 failure was greatest with *Gloeophyllum trabeum*.

Evaluation of the macroscopic failure data confirmed that decayed wood (> 2% weight loss) failed in a different manner than sound wood.

#### Ultrastructural features

*Sound wood.* - Transwall failure of fibers at angles close to the S2 microfibrillar orientation (Fig. 4) and intrawall failures at the S1/S2 interfaces (Figs. 5 and 6) were

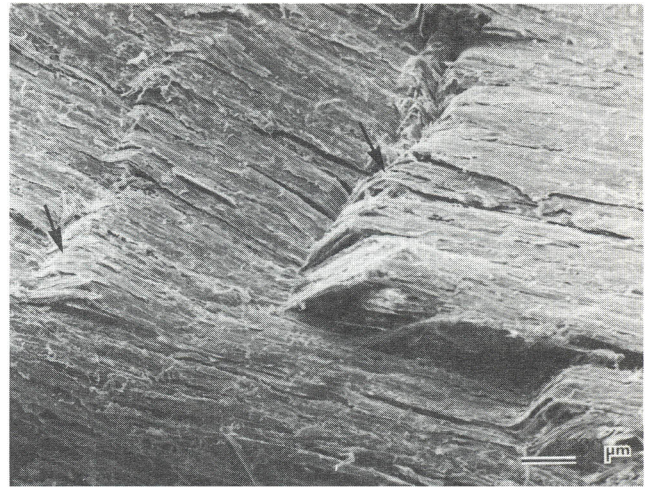


Figure 3. - Micrograph showing compression ridges (arrows) resulting from cell buckling on the compression side of a sound toughness test specimen following an impact load. Micrograph was taken from a Type 2 failure sample.

Figure 4. - Micrograph of sound wood fibers showing transwall (tw) failures along the 82 microfibrillar angle (arrow). The lumen (Lu) was generally exposed during transwall failures. Micrograph was taken from Type 1 fracture plane of a tension specimen.

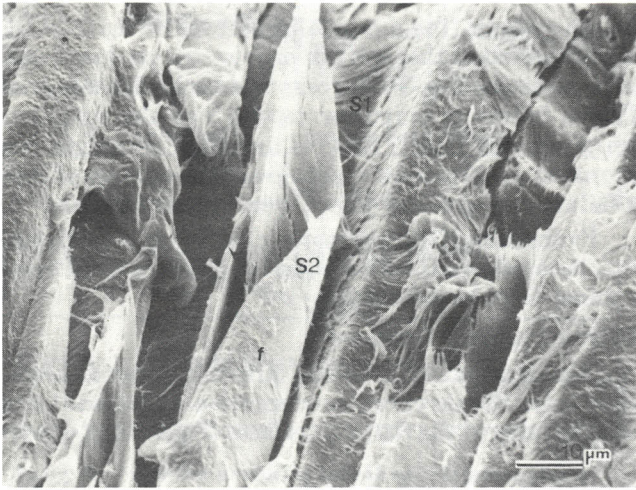


Figure 5. - Micrograph of a sound wood tangential fracture plane showing an unwinding phenomenon (arrow) of a fiber (f) as intrawall failure took place at interface between S1 and S2 layers. The S2 layer was pulled out of the cell during this process. Micrograph was taken from Type 3 fracture plane of a tension specimen.

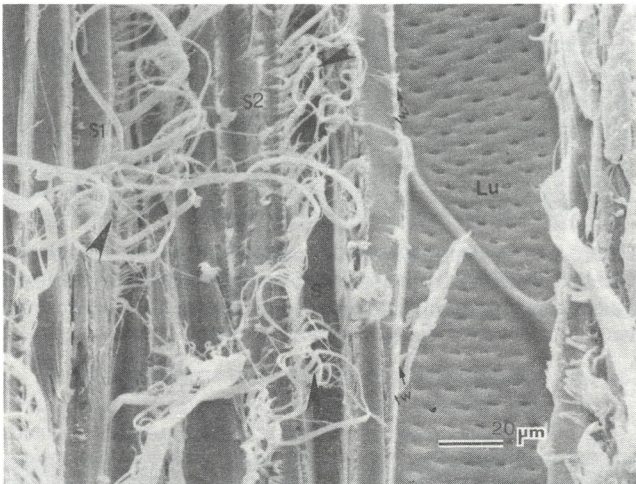


Figure 6. - Micrograph of a tangential fracture plane in sound wood. Intrawall failure of fibers (arrows) occurred within either the S1 or the S2 wall layers or at their interfaces (S1/S2). The vessel lumen (Lu) was left intact but the vessel walls generally failed in a transwall manner. Micrograph was taken from Type 3 fracture plane of a toughness specimen.

dominant within Type 1, 2, and 3 failure categories. Intra-wall failure of fibers was usually prominent on the tangential fracture plane. Figure 5 shows that this type of failure can unwind the fiber, causing the S2 wall layer to pull out of the whole cell. In sound wood, the vessel walls generally failed in a transwall manner (Fig. 6) while the fibers exhibited intra wall failure within the S1 or S2 wall layers, at, or close to their interface. Figure 7 shows that sound wood fiber failures in tension were generally transwall along the S2 microfibrillar angle. In addition, intercellular failures occurred at the ray/fiber interfaces.

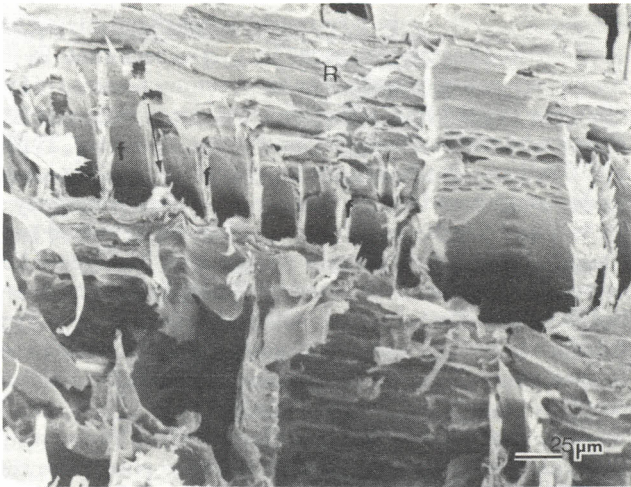


Figure 7. - Micrograph of a radial-longitudinal fracture plane in sound wood. The fibers (f) generally failed at steep angles (arrow) close to the S2 microfibrillar orientation. The ray/fiber interface (R) appears to be a weak plane where intercellular fractures occurred. Micrograph was taken from Type 1 fracture plane of a tension specimen.

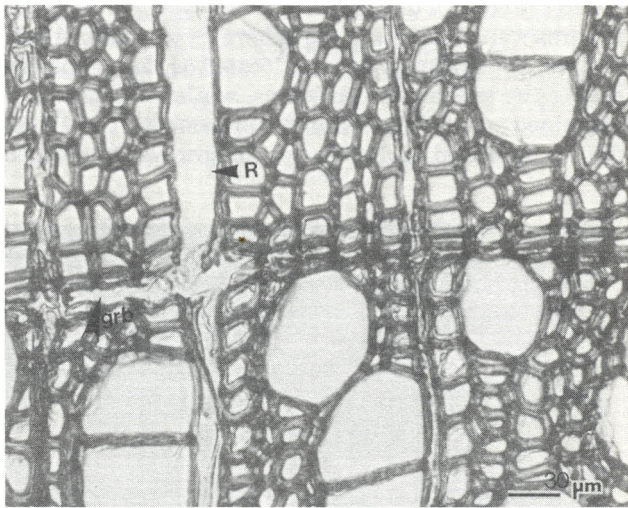


Figure 8. - Light micrograph showing a cross-sectional view of aspen decayed by *Trametes versicolor*. Observe enlarged flaw developments along the growth ring boundary (grb) and region of the rays (R). Micrograph was obtained from a toughness specimen at 7 percent weight loss.

decayed by all the test fungi had their longitudinally oriented cells fail along the 82 microfibrillar angle, just as the sound wood cells failed. At 7 percent weight loss, wood decayed by *Bjerkandera adusta* and *Trametes versicolor* showed enlarged flaw development (Fig. 8) along the growth ring boundaries and ray zones. Fracture planes through these two sites are depicted in Figure 9. Transmission micrographs taken of the cross sections of the same white-rotted aspen revealed that Type 5 failures originated from transwall fractures that propagated along degraded parenchyma cells (2). In this study, fracture surfaces produced from *Bjerkandera adusta* decay were similar to those pro-

3. duced by *Trametes versicolor*. Wood decayed beyond 2 percent weight loss by all three fungi had some cells that failed in an abrupt transwall fashion (Figs. 9, 10, and 11) across the transverse plane. Such failures did not follow the S2 microfibrillar orientation and they occurred more frequently in cells located close to the specimen exterior. At a weight loss over 10 percent, abrupt transwall fiber failure (Fig. 12) along the transverse plane (which resulted in Type 4 failure) appeared to be more common. Type 4 failure was the primary failure in wood decayed by *Gloeophyllum trabeum*, which produced both transverse and longitudinal failures (Types 4 and 5).

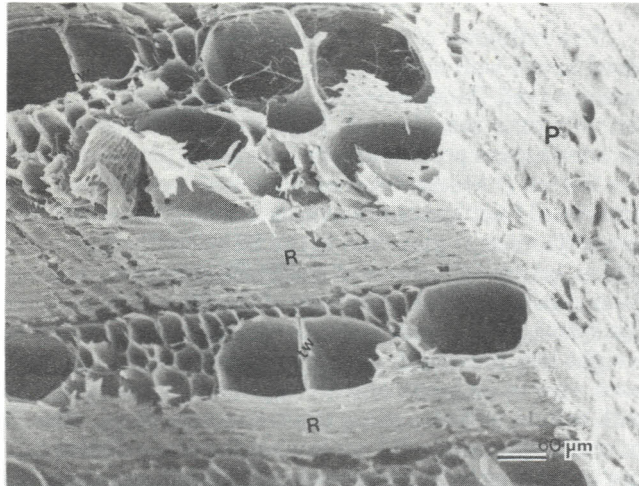
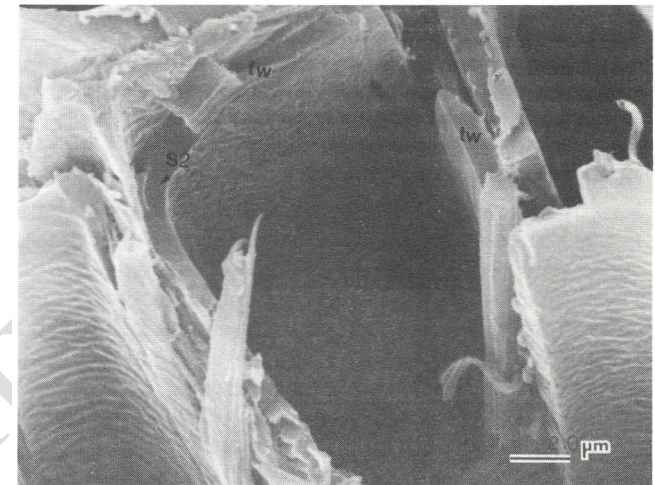


Figure 9. - Micrograph showing planes of failure (P) and (R) along the growth ring boundary (containing marginal parenchyma) and ray parenchyma, respectively. Most of the longitudinally oriented cells failed in an abrupt transwall (tw) manner. Micrograph was obtained from Type 5 fracture plane of a toughness specimen decayed by *Trametes versicolor* to 10 percent weight loss.



and appeared not to be influenced by the 82 microfibrillar orientation. Micrograph was obtained from Type 4 fracture plane of a toughness specimen.

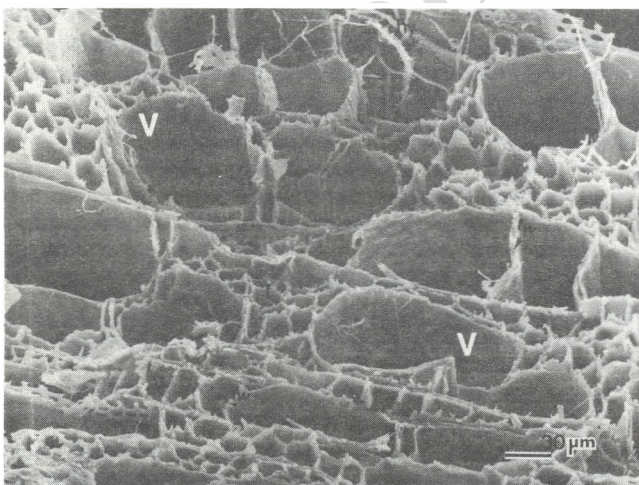
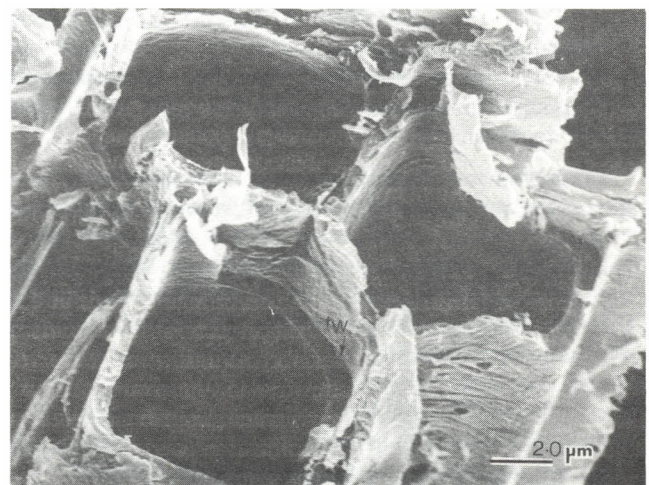


Figure 10. - Micrograph of transverse fracture plane in wood decayed by *Gloeophyllum trabeum* to 6 percent weight loss. Abrupt transwall (tw) failure of vessels (V) and fibers (1) occurred



### Discussion

Brashness is a brittle failure phenomenon occurring abruptly from cracks that propagate at low energy levels (1). The low energy required for wood to fail is of general concern to wood scientists because this can lead to structural collapse. When wood is sound, associated failure types are generally characterized by large deformation responses including splintering and production of rough shear planes. This is because the S2 wall layer resists much of the load in tension to produce transwall failure of fibers at angles close to the S2 microfibrillar orientation. Cellular unwinding sometimes occurred due to intrawall failures, whereby the S2 layer was pulled out of other cell wall layers. During this process, slippage probably occurred between the microfibrils to cause intrawall failure at

Figure 11. - Micrograph showing an abrupt transwall (tw) fiber failure in wood decayed by *Bjerkandera adusta* to 6 percent weight loss. Transwall failure occurred despite the relatively thick S2 layer in this decayed cell. Micrograph was obtained from Type 4 fracture plane of a toughness specimen.

Figure 12. - Micrograph showing abrupt transwall (tw) fiber failures in wood decayed by *Gloeophyllum trabeum*. Micrograph was obtained from Type 4 fracture plane of wood decayed to 16 percent weight loss before tension test.

Bowen University IR

the 81/82 interface while the fiber core pulled out of the cell. The ray/fiber interface was a recognized weak zone during wood failure (6) and this may explain why tension loads were generally accommodated by the longitudinally oriented fibers. Vessel failures were generally transwall, while fiber failures often combined both transwall and intrawall failure modes. When intercell failures occurred, they were usually at interfaces between rays and fibers. All of these failures occurred simultaneously, making the wood cells readjust and realign to accommodate applied stresses. Ultimate failure is believed to have occurred when imposed stresses exceeded these internal resistances. Rough fracture surfaces therefore resulted, presumably with large surface areas.

High-energy failure patterns in wood retained their integrity up to 2 percent weight loss. This trend agrees with the nonsignificant difference in results obtained by analyzing macroscopic failures in sound and decayed woods

at this level of decay. At weight losses greater than 2 percent, some of the wood cells were already weakened and a considerable amount of their resistance to crack development had been lost. Large deformation patterns characteristic of sound wood failure attenuated as decay progressed. Transverse brash failures and longitudinal smooth splits emerged as new macroscopic features of failure. Their effect became dominant beyond 10 percent weight loss and this probably made any difference in failure types, caused by the different fungi, nonsignificant at this stage. At the microscopic level, abrupt transwall failures of the longitudinally oriented elements were apparent and the 82 microfibrillar orientation lost its influence in dictating fiber failure angles. This is probably because the cellulose chains were already depolymerized by fungal enzymes. Brown-rot fungi have been reported to depolymerize cellulose more rapidly than they can metabolize the degradation products at early stages of decay (7,8). This could account for the high incidence of abrupt transwall (transverse) failures found with *Gloeophyllum trabeum* decay. White-rot fungi, on the other hand, depolymerize cellulose slowly and simultaneously utilize the degradation products (14). The presence of fibers that broke abruptly under *Bjerkandera adusta* attack highlights the tendency for white-rot fungi to remove all the cell wall components, even though this particular fungus may show preferential lignin degradation.

Degradation of parenchyma cells is believed to be an important part of weight loss and fracture development in aspen exposed to white rot. The smooth longitudinal split fracture planes were generated from transwall failures along degraded marginal parenchyma cells. Because they are storage cells, parenchyma may contain readily available carbohydrates that could provide an initial food source, not only for white rot but also brown rot. However, it is possible that the widely dispersed nature of the cellulolytic system of brown-rot fungi overshadowed any localized degradation and fracture development.

Results from this study indicate that fracture surfaces created under the influence of *Trametes versicolor* were similar to those created by *Bjerkandera adusta*. This might

be due to the fact that both fungal species removed lignin and carbohydrate wood fractions regardless of the pattern

and rate of removal. It is also not certain, under the present experimental conditions, whether *Bjerkandera adusta* acted as a selective delignifier. For example, it was expected that middle lamella separation (intercellular failure) would be a prominent fractographic feature with this fungus, which was reported to be capable of causing preferential lignin degradation (3). Middle lamella separation probably requires a greater level of delignification than was achieved by 16 percent weight loss. It is therefore assumed the critical flaws that led to longitudinal smooth splits in decayed wood began at weight losses below those required to produce middle lamella separations.

### Conclusions

The influence of fungal decay on wood failure is related to cell wall degradation and the amount of weight loss incurred. Decayed wood (> 2% weight loss) failed differently than sound wood. High-energy fracturing, like splintering and production of rough shear planes, typified the failure characteristics at 2 percent weight loss. The associated fractographic features included transwall failure of fibers at angles close to the 82 microfibrillar orientation, intrawall failures at the 81182 interfaces, and cellular unwinding due to pullout of the 82 wall layer from the whole fiber. These features diminished gradually as weight loss increased. At ~ 10 percent weight loss, failures were often brash and accompanied by abrupt transwall failure of fibers along the transverse plane. The 82 microfibrillar angle did not control the plane of fiber failure in decayed cells. Longitudinal split failures along the parenchyma cells were frequently noted on specimens decayed by white-rot fungi. Such failures were initiated at weight losses lower than those required to produce middle lamella separation.

From this work, it is confirmed that wood embrittlement resulting from decay is associated with certain microfibre failure patterns. Abrupt (transverse) transwall fiber failures occurred to reduce resistance of wood cells in axial tension, while longitudinal transwall failures along white-rotted parenchyma cells resulted in smooth split fracture surfaces and a probable reduction in shear resistance. All these features represent defects in wood structure that encourage brash failures.

### Literature cited

5. Akande, J.A. 1988. Effect of decay on strength and fracture morphology of *Populus tremuloides* Michx. Ph.D. thesis. SUNY ESF, Syracuse, N.Y. pp. 1-183.
2. , G.H. Kyanka, and RB. Hanna. 1990. Development of longitudinal split failure in white-rotted aspen (*Populus tremuloides* Michx), *Wood and Fiber Sci.* 22(4): .
3. Blanchette, RA., 1. Otjen, M.J. Efland, and W.E. Eslyn. 1985. Changes in structural and chemical components of wood delignified by fungi. *Wood Sci. Technology* 19:35-46.
4. Cartwright, K.G., W.P.K. Findlay, C.J. Chaplin, and W.G. Campbell. 1931. The effect of progressive decay by *Trametes serialis* Fr. on the mechanical strength of the wood of sitka spruce. Great Britain Dept. Sci. Ind. Res. Forest Prod. Res. Bull. No.11.
5. and . 1950. Decay of timber and its prevention. Forest Prod. Res. Lab., Chemical Publishing Co., Brooklyn, N.Y. 294 pp.

6. Cote, W.A. and RB. Hanna. 1983. Ultrastructural characteristics of wood fracture surfaces. *Wood and Fiber Sci.* 15(2):135-163.

JULY/AUGUST 1990

7. Cowling, E.B. 1961. Comparative biochemistry of the decay of sweetgum sapwood by white rot and brown rot fungi. USDA Tech. Bull. No. 1258. Washington D.C.
8. . 1965. Chemical modification of wood during microbial deterioration. *Holz und Organismen (Supplnt. to Material und Organismen)* (1):91-102.
9. Otjen, L. and RA. Blanchette. 1985. Selective delignification of aspen wood blocks in vitro by three white rot basidiomycetes. *Applied Environmental Microbiology* 50(3):568-572.
10. Panshin, A.J. and C. deZeeuw. 1980. *Textbook of Wood Technology*. McGraw Hill Book Co., N.Y. pp. 358-404.
11. Scheffer, T.C. 1936. Progressive effect of *Polyporus versicolor* on the physical and chemical properties of redgum sapwood. USDA Tech. Bull. No. 527.
12. . 1982. Effect of decay on physical properties. *In: Wood Deterioration and its Prevention by Preservative Treatments*. Vol. 1. D.D. Nicholas, ed. Syracuse Univ. Press, Syracuse, N.Y. 380 pp.
13. Toole, E.R 1969. Effect of decay on crushing strength. *Forest Prod. J.* 19(10):36-37.
14. Wilcox, W.W. 1973. Degradation in relation to wood structure. *In: Wood Deterioration and its Prevention by Preservative Treatments*. Vol. 1. D.D. Nicholas, ed. Syracuse Univ. Press, Syracuse, N.Y. 380pp.

Bowen University IR

Bowen University IR